Original Article

Metformin suppresses vascular smooth muscle cell senescence by promoting autophagic flux

Shi Tai [a,1], Jiaxing Sun [a,1], Yuying Zhou [b], Zhaowei Zhu [a], Yuhu He [a], Mingxian Chen [a], Hui Yang [a], Yichao Xiao [a], Tao Tu [a], Liang Tang [a], Xuping Li [a], Jianping Zeng [b], Xilong Zheng [c], Shenghua Zhou [a,*]

[a] Department of Cardiovascular Medicine, the Second Xiangya Hospital of Central South University, Changsha 410011, China
[b] Department of Cardiovascular Medicine, Xiangtan Central Hospital, Xiangtan 411100, China
[c] Department of Biochemistry & Molecular Biology, University of Calgary, Calgary T2N 4N1, Canada

HIGHLIGHTS

- Metformin treatment improved functional and structural changes occur in aging arteries.
- Metformin treatment prevented a senescence-associated secretory phenotype and improved the proliferation and migration of senescent VSMCs.
- Reduced autophagic flux during cellular and vascular senescence was reversed by metformin.
- Metformin enhances autophagy flux at the level of autophagosome-lysosome fusion via upregulating LAMP1.

GRAPHICAL ABSTRACT

Our data suggest that metformin regulates the level of autophagosome-lysosome fusion leading to the upregulation of autophagic flux and significantly alleviates functional and structural changes associated with aging arteries, such as collagen accumulation and elastin damage. Metformin treatment also prevents a senescence-associated secretory phenotype (SASP) and improves the proliferation and migration of senescent VSMCs. Furthermore, disrupting the autophagosome-lysosome fusion abrogates the anti-senescence effects induced by metformin in VSMCs. Autophagy process is complex and involves multiple steps, it is unknown whether p62 mediated-selected autophagy seen in metformin treatment also contributes to activation of autophagic flux. Altogether, metformin, as an anti-aging drug, together with its novel role, as a regulator of autophagic flux, contributes to reduced senescence and SASP of VSMCs.
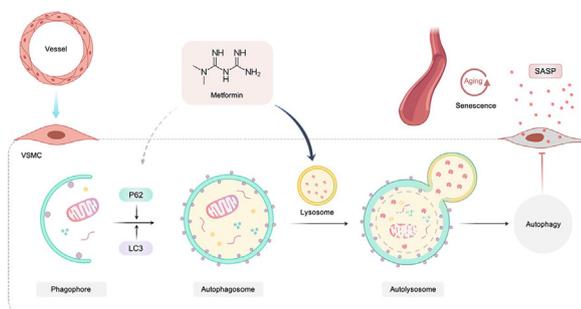
ARTICLE INFO

ABSTRACT

Introduction: Vascular smooth muscle cell (VSMC) senescence in the vasculature results in vascular aging as well as age-related diseases, while metformin improves the inflamm-aging profile by enhancing autophagy. However, metformin's impact on VSMC senescence is largely undefined.
Objectives: To test the hypothesis that metformin exerts an anti-senescence role by restoring autophagic activity in VSMCs and vascular tissues.
Methods: Animal models established by angiotensin II (Ang II) induction and physiological aging and senescent primary VSMCs from the aortas of elderly patients were treated with metformin. Cellular

---

and vascular senescence were assessed by measuring the amounts of senescence-associated β-galactosidase and senescence markers, including p21 and p53. Autophagy levels were assessed by autophagy-related protein expression, transmission electron microscope, and autolysosome staining. In order to explore the underlying mechanism of the anti-senescence effects of metformin, 4D label-free quantitative proteomics and bioinformatic analyses were conducted, with subsequent experiments validating these findings.

Results: Ang II-dependent senescence was suppressed by metformin in VSMCs and vascular tissues. Metformin also significantly improved arterial stiffness and alleviated structural changes in aged arteries, reduced senescence-associated secretory phenotype (SASP), and improved proliferation and migration of senescent VSMCs. Mechanistically, the proteomic analysis indicated that autophagy might contribute to metformin's anti-senescence effects. Reduced autophagic flux was observed in Ang II-induced cellular and vascular senescence; this reduction was reversed by metformin. Specifically, metformin enhanced the autophagic flux at the autophagosome-lysosome fusion level, whereas blockade of autophagosome-lysosome fusion inhibited the anti-senescence effects of metformin.

Conclusions: Metformin prevents VSMC and vascular senescence by promoting autolysosome formation.

Introduction

Metformin is a biguanide capable of relieving age-associated pathologies and increasing healthspan and was the first tested product showing aging-targeting effects in a clinical study with a large sample: the TAME (targeting aging by metformin) study [1]. Several studies have demonstrated that metformin could alleviate aging and age-related phenotypes [2–4] by suppressing senescence through mechanisms like redox balance, autophagy, inflammatory cytokines, and endothelial function [5–9].

Cellular senescence represents a well-defined phenotype featuring irreversible cell cycle arrest [10–12] and acquired senescence-associated secretory phenotype (SASP) [13]. SASP is associated with various adverse effects caused by proinflammatory factors, matrix metalloproteinases, and growth factors [14,15]. Accumulation of senescent cells and secretion of proinflammatory factors in the aging vasculature could lead to altered vasodilation, chronic inflammatory response and pathologic extracellular matrix (ECM) remodeling, causing vascular dysfunction [16] and age-related diseases [17]. Recent studies found that the accumulation of senescent VSMCs can result from defective autophagy [18,19], and blockage of autophagic flux can enhance senescence in VSMCs [20], suggesting that reduced autophagy might induce senescence.

Autophagy is a highly-conserved process with major roles in cell homeostasis and survival and has been implicated in increased susceptibility to cardiovascular disorders upon aging [21,22]. A recent study reported that metformin enhances autophagy and improves mitochondrial function while ameliorating the inflamm-aging profile mimicking the inflammatory response in diabetes.[6] Nevertheless, metformin's impact on VSMC senescence remains undefined. We hypothesized that metformin exerts anti-senescence effects by restoring autophagic activity in VSMCs and vascular tissues.

Methods

Animals

Male C57BL/6 mice (10 weeks old, 25–30 g) from Hunan SJA Laboratory Animal (China) underwent housing at 22 ± 2 °C under a 12 h-12 h light/dark cycle with freely available rodent chow and water. The animals were randomized into the saline-infusion, saline-infusion + metformin, Ang II-infusion, and Ang II-infusion + metformin groups. Anesthesia was carried out with 1% isoflurane and 99% oxygen at 20 mL/min. A micro-osmotic pump

(Alzet model 2004; AlzaCorp, USA) with either saline or Ang II in saline (400 ng/kg/min for 28 days) was implanted subcutaneously into each mouse under sterile procedures. The mice in the metformin and Ang II-infusion + metformin groups received metformin (150 mg/kg/d) by intragastric administration once a day for 28 days from day 1 after pump implantation. In addition, aging mice were used to test the effects of metformin. Male C57BL/6 mice were divided into three groups: 10 months (control) group, 20 months (old) group, and old + metformin group to receive water or 3 g/l metformin in water (a dose proved to elicit clinically relevant serum metformin concentration) [23] for 10 months. The administration of metformin began at 10 months of age and continued for 10 months until the mice were 20-month-old.

Ethics statement

All experiments involving animals and clinical samples were conducted according to the ethical policies and procedures approved by the ethics committee of the Second Xiangya Hospital of Central South University. The need for individual consent was waived by the committee. (Approval no. 2018.200).

Blood glucose and noninvasive blood pressure measurements

The effect of metformin on glucose levels was evaluated. Blood glucose levels were measured by a tail nick using a glucometer (EA-11, Sinocare, China). In order to monitor the blood pressure after implantation of the Ang II infusion pump, noninvasive blood pressure in mice was measured by the computerized tail-cuff method (CODA 6, Kent Scientific, USA). In a 3-day adaptive period, the animals underwent training in pre-warmed tail-cuff devices. Blood pressure was measured at least 20 times in each mouse until it reached a steady-state, and the final value was obtained from an average of 10 proximal repeats.

Pulse wave velocity (PWV) assessment

PWV reflects arterial wall stiffness, providing a simple and accurate tool for quantifying arterial stiffness *in vivo*: the stiffer the artery, the elevated the PWV [24]. Noninvasive aortic PWV measurement in mice was conducted as previously described [25]. Briefly, anesthesia was followed by animal placement in the supine position with paws taped to electrodes on an ECG board. A 20-MHz Doppler probe was utilized for recording velocity in the aortic arch moving away from the probe at 2 to 4-mm depth.

A mark was made 30–40 mm distally on the abdomen. A measurement was taken at the mark from the abdominal aorta, with the probe angled toward the heart at a depth of 2–3 mm. Aortic PWV was calculated by dividing the separation distance (30–40 mm) by the difference in arrival times of the velocity pulse timed with respect to the ECG. After PWV evaluation, the mice were euthanized with 1% pentobarbital (30 mg/kg) by intraperitoneal injection at 28 days after micro-osmotic pump implantation, and aortas were harvested for subsequent analyses.

Histological analysis and immunohistochemistry

Changes in collagen and elastin amounts or aortic wall arrangement were evaluated by histology. Tissues underwent perfusion-fixation with 4% formalin, paraffin embedding, and 5 μm sectioning, followed by Masson's trichrome, Sirius red, and Van Gieson staining with kits from Servicebio (China), following the manufacturer instructions. Masson's Trichrome staining was used to visualize the overall aortic morphology and architecture. Picrosirius red staining under circularly polarized light was used to visualize collagen. Van Gieson's staining was used to visualize elastin within the aortic wall. Tissue dimensions and collagen were determined within each ring by direct pixel quantification using Image-Pro Plus (Media Cybernetics, Georgia). Collagen contents were computed for the entire tissue ring by proportioning the sampled area to the total tissue area. Optical densities were computed by normalizing the content within a field to the underlying area of tissue within that field [26].

Immunohistochemical analysis was carried out to detect p53 and p21 expression in all groups. Briefly, xylene dewaxing was followed by rehydration in a stepwise manner using ethyl alcohol and antigen retrieval for 10 min at 120 °C. After a 30-min incubation at room temperature (20 °C–25 °C) with blocking buffer, the sections underwent overnight incubation with primary antibodies raised against p21 (Proteintech, USA, #10355–1-AP; 1:600) and p53 (Proteintech, #10442–1-AP; 1:100) at 4 °C. Next, secondary antibodies (Proteintech, #SA00004-1 and #SA00004-2; 1:100) were added at ambient for a 30-minute incubation. After development with the DAB solution, hematoxylin counterstaining was performed before imaging under an Olympus microscope (Japan). Image J (National Institutes of Health, USA) was utilized for quantitation, and values for four sections were averaged.

Immunofluorescence

Immunofluorescence was used to detect autophagy markers in aortas from mice. After antigen retrieval, tissue sections were incubated overnight with antibodies against α-SMA (Abcam, UK, ab7817; 1:100), LC3B (Cell Signaling Technology [CST], USA, #3868; 1:100), and p62 (CST, #39749s; 1:100) at 4 °C. Then, goat anti-mouse or anti-rabbit fluorescein isothiocyanate (FITC) or tetramethyl-rhodamine isothiocyanate (TRITC)-linked secondary antibodies (1:100) were added for a 1-h incubation at 37 °C. The sections then underwent counterstaining with DAPI. A nonspecific IgG-stained section served as a negative control. Imaging was performed with an Olympus microscope (×200 magnification). Color composite images were generated and analyzed using the Image J software.

4D label-free quantitative proteome analysis

Proteomics was conducted to explore the mechanism by which metformin exerts anti-senescence effects. C57BL/6 mice were randomly assigned to the saline control, Ang II infusion, and Ang II infusion + metformin groups. The mice in the metformin and Ang

II infusion + metformin groups received metformin (150 mg/kg/d) by intragastric administration once daily for 28 days from day 1 after micro-osmotic pump (400 ng/kg/min for 28 days) implantation. Euthanasia was performed with 1% pentobarbital (30 mg/kg) by intraperitoneal injection, and the aortas from the mice were arvested on day 28. Protein extraction and trypsin digestion were conducted, followed by LC-MS/MS. The MaxQuant search engine (v.1.6.15.0) was used for MS/MS data analysis. FDR was adjusted to < 1%.

Cell culture and isolation of primary VSMCs

VSMCs were provided by Shanghai cell bank and cultured in Dulbecco's modified eagle medium (DMEM)-F12 medium (Thermo Fisher Scientific, #C11330500BT) containing 100U/ml penicillin, 100 μg/ml/ml streptomycin (Thermo Fisher Scientific, #15140122), and 10% fetal bovine serum (FBS, Gibco, #10099-141). Stress-induced premature senescence in VSMCs was triggered by Ang II treatment (2 μM) for 72 h.

Primary human aortic smooth muscle cells were isolated from the aortas of elderly patients with aortic dissection undergoing aortic replacement surgery, according to a previously described method [27]. Briefly, the aorta was isolated with fat tissues and the adventitia removed, and the intima was scraped. The aorta was cut into approximately 1-mm blocks and cultured for about 2 h before the addition of DMEM-F12 medium (Thermo Fisher Scientific, #C11330500BT) with 20% FBS for a 5-day culture. Primary VSMCs that started to expand were further cultured in DMEM-F12 medium containing 10% FBS and penicillin/streptomycin for subsequent experiments. Primary VSMCs derived from individual patients were not pooled. Primary VSMCs were studied at passages 2–10 or until replicative senescence was reached. It is known that the expression of α-SMA and SM22α will dominate in senescent smooth muscle cells [28]. We therefore performed the immunofluorescence staining on isolated VSMCs with senescence, results showed that the rate of α-SMA or SM22α positive cells is above 95% (Supplementary Fig. 2), thus our data inferred that corrected VSMCs were isolated.

Senescence-associated β-galactosidase (SA-β-gal) staining

Ang II-induced senescent VSMCs pretreated with or without metformin (200 μM) for 2 h were incubated with Ang II for 72 h and then stained using an SA-β-gal staining kit (Beyotime, China; C0602). Senescent primary VSMCs were treated with metformin (200 μM) for 12 days, also with medium change and re-intervention every 24 h, followed by SA-β-gal labeling. After three PBS washes, the cells underwent fixation (fixation buffer) for 15 min and overnight incubation with freshly prepared SA-β-gal staining solution (pH 6.0) at 37 °C. For histological assessment, vascular samples were fixed with the fixation buffer for 20 min and underwent overnight incubation in SA-β-gal staining solution at 37 °C for 18 h. The proportion of SA-β-gal-positive cells based on the total number of cells was determined.

Western blot analysis

Whole cells were collected and lysed using the radioimmuno-precipitation assay (RIPA) buffer. Protein separation utilized 12.5% sodium dodecyl sulfate (SDS)-polyacrylamide gel electrophoresis (PAGE). The protein bands were electro-transferred onto polyvinylidene fluoride (PVDF) membranes. Following blocking (5% fat-free milk), overnight incubation with primary antibodies targeting LC3 (CST, #3868; 1:1,000), p53 (Proteintech, #10442-1-AP; 1:2,000), p21 (Proteintech, #10355-1-AP; 1:1,000),

p62 (Proteintech, #18420-1-AP; 1:2,000), p16[INK4] (CST, #80772 s; 1:1,000), IL-6 (CST, #12912; 1:1,000), MMP-2 (Proteintech, #10373-2-AP; 1:1,000), TGFβ (CST, #37111 s; 1:1,000), PCNA (CST, #13110 s; 1:1,000), SM-22α (Abcam, #ab14106; 1:1,000), Calponin (Abcam, #ab46794; 1:1,000), LAMP1 (Abcam, #ab108597; 1:1,000), CTS-L(Santa Cruz, #sc-32320; 1:500), CTS-B (Boster, #BM5040; 1:1,000) and GAPDH (Proteintech, #60004-1-Ig; 1:3,000) was carried out at 4 °C overnight. After incubation with the corresponding secondary antibodies (Proteintech, #SA00001-1 or #SA00001-2; 1:5,000), enhanced chemiluminescence (Bio-Rad, USA) was used to detect immunoreactive bands. Image J was utilized for quantitation.

Wound-healing assay

Metformin's effect on VSMC migration was assessed by the wound-healing assay. After confluent growth of VSMCs in a 6-well plate, cells underwent serum starvation for 24 h. Then, monolayer scratching was carried out using a 200-μL pipette tip. Cells were then stimulated with Ang II or metformin in DMEM-F12 supplemented with 1 % FBS. Wound healing was imaged at the indicated time points after scratching and quantified at a fixed location using Image-Pro Plus. Data from four independent experiments were analyzed.

Cell cycle analysis

Metformin's effect on the proliferation of VSMCs was assessed by cell cycle analysis, flow-cytometrically following propidium iodide (PI) staining. Briefly, 1×10^6 cells underwent fixation for 2 h with 70% alcohol at 4 °C and treatment with PI solution (MCE, USA; #HY-D0815) at 50 μg/ml containing 0.6 μl RNase A (20 μg/ml) in the dark for 30 min at 4 °C. At least 2,000 cells were analyzed per sample, using Flow Jo 7.0 (Flow Jo, USA). Data from three independent experiments were analyzed.

Autolysosome staining

In order to evaluate the effect of metformin on autophagic flux, autolysosome staining was performed. After seeding in 6-well glass-bottom plates, the VSMCs underwent overnight culture at 37 °C with 5% CO$_2$. After incubation with 1 mL DAL Green (l μmol/L) working solution for 30 min, the cells were cultured with or without Ang II or metformin for 6 h. Following two PBS washes, a laser confocal microscope (Carl Zeiss, Germany) was utilized for analysis.

Adenovirus transfection

VSMCs were transfected with Ad-control or Ad-sqstm1/p62-RNAi (100 MOI, Shanghai Genechem Co., Ltd.) in a medium without FBS for 2 h, washed with PBS twice, and cultured in a medium with 10% FBS for 24 h. Then, the cells were stimulated with Ang II with or without pre-incubation of metformin for 24 h. The cells were collected for western blot analysis.

Statistical analysis

Data collected from ≥ 3 independent assays were presented as mean ± standard deviation (SD). GraphPad Prism v8.0 (GraphPad, USA) was utilized for data analysis. Normally distributed data were compared using *t*-test and one-way analysis of variance (ANOVA) with Tukey's post hoc test for group pairs and multiple groups, respectively. Non-normally distributed data were compared using the Mann-Whitney *U* test and the Kruskal-Wallis test for group pairs and multiple groups, respectively. $P < 0.05$ was considered statistically significant.

Results

Metformin prevents vascular senescence

In order to determine whether metformin protects against senescence in vascular tissues, the mice were randomized into the saline-infusion, saline-infusion + metformin, Ang II-infusion, and Ang II-infusion + metformin groups. According to Li. et al., [29] chronic Ang II infusion by micro-osmotic pump (400 ng/kg/min for 28 days) results in vascular senescence. In addition, the metformin doses used *in vivo* and *in vitro* were according to previous studies [5,30]. Thus, mice subjected to chronic Ang II infusion underwent treatment with or without metformin [30] (150 mg/kg/d by intragastric administration once daily for 28 days from day 1 after pump implantation). Consistent with a previous report [29], chronic Ang II administration (400 ng/kg/min) elevated systolic blood pressure in mice on days 14 and 28, whereas metformin had no effects on blood pressure in the saline and Ang II-infusion groups. In addition, blood glucose levels were comparable in the Ang II-infusion + metformin and Ang II-infusion groups (Supplementary Fig. 1). Next, vascular senescence was examined by SA-β-gal staining and quantitating p53 and p21 expression. Aorta specimens from Ang II-infused mice displayed significantly higher SA-β-gal staining compared with the saline group (Fig. 1A, upper and middle panels). In Ang II-infused mice, metformin strongly decreased aortic SA-β-gal activity compared with non-metformin-treated animals (Fig. 1A, upper and middle panels). Similarly, metformin decreased SA-β-gal activity in aortas from aging mice (Fig. 1A, lower panel). Immunohistochemical staining revealed that p53 and p21 levels were increased in aortas (mainly in the tunica media) from the Ang II group in comparison with the saline group; however, the Ang II infusion + metformin group displayed lower p53 and p21 levels than the Ang II infusion group (Fig. 1B-C). These results were further confirmed by Western blot (Fig. 1 D-F). Meanwhile, metformin significantly decreased aortic SA-β-gal activity and p53 and p21 levels in Ang II-infused animals, but not saline-infused mice.

Arterial stiffness represents the earliest detectable manifestation of the deleterious changes of a vessel wall structure and function [24,31]. Enhanced stiffness of large conduit arteries represents an important indicator of vascular senescence [16,32]. PWV measurement constitutes a valid tool for noninvasive quantitation of arterial stiffness [31]. As expected, PWV was higher in Ang II infused animals in comparison with age-matched control mice, while metformin significantly decreased PWV in comparison with the Ang II group (Fig. 2 A and B; Supplemental Table 1). Various structural alterations occur in the aging artery, including elastin fragmentation, enhanced collagen production, and medial VSMC loss, resulting in decreased vascular compliance and enhanced arterial stiffness [33]. Therefore, we evaluated the changes in collagen and elastin contents as well as aortic wall arrangement by staining aortic tissue rings with Masson's trichrome, Picrosirius red, and Van Gieson stains. Morphometric analysis of the four groups was performed after Masson's trichrome staining (Fig. 2C). Aortas in the Ang II-infusion group displayed greater lumen diameters and medial layer thicknesses than those of the saline-infusion group, and medial thicknesses were markedly reduced in the Ang II-infusion + metformin group compared with the Ang II-infusion group (Fig. 2C, F, H, and I). Similarly, medial cross-sectional areas were starkly greater in the Ang II-infusion group versus the saline-infusion group but lower in the Ang II-infusion + metformin group compared with the Ang II-infusion group
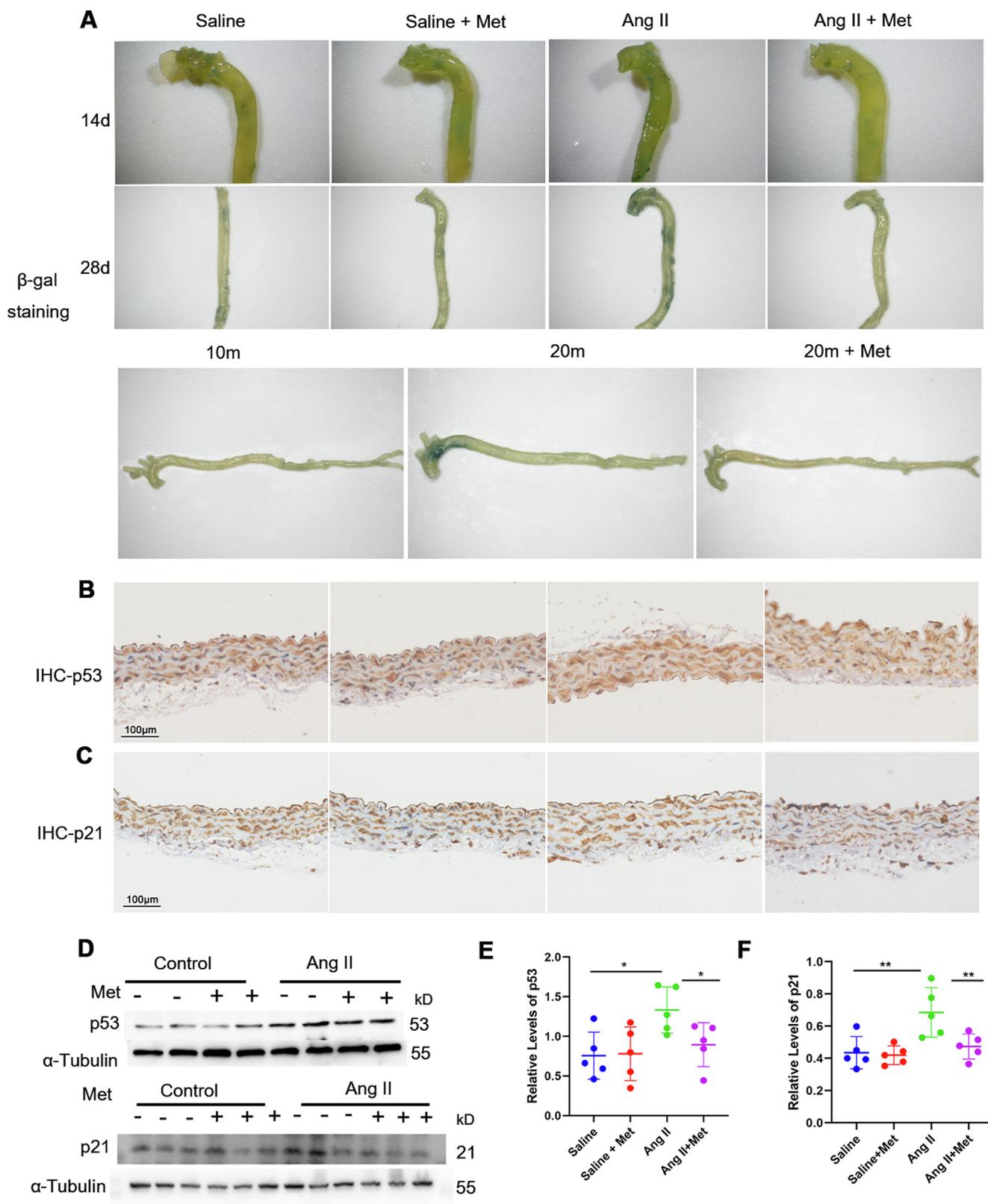
Fig. 1. Metformin prevents vascular senescence. Mice underwent infusion with saline (control), saline + metformin (150 mg/kg/d), Ang II (400 ng/kg/min) and Ang II (400 ng/kg/min) + metformin (Met, 150 mg/kg/d) with an Alzet osmotic minipump for 14 or 28 days, respectively. **A, Upper and middle panels**, SA-β-gal staining (positive β-galactosidase staining appears blue) was carried out for assessing senescence of the mouse aorta (14 and 28 days, respectively). **A, Lower panel**, SA-β-gal staining of aortas from physiological aging mice (n = 3); 10-month-old, 20-month-old, 20-month-old + metformin. **B and C**, Immunohistochemistry was performed to detect p53 and p21 in aorta samples from 4 groups (n = 3); scale bar = 100 μm. **D, E, and F**, Immunoblot was performed to assess p53 and p21 protein levels in aorta samples from the four groups (one-way ANOVA, Tukey post hoc; n = 5). α-tubulin was utilized for normalization. Data are mean ± SD. *P < 0.05, **P < 0.01, and ***P < 0.001 versus control group or for indicated comparisons. Met, metformin; Ang II, angiotensin II.
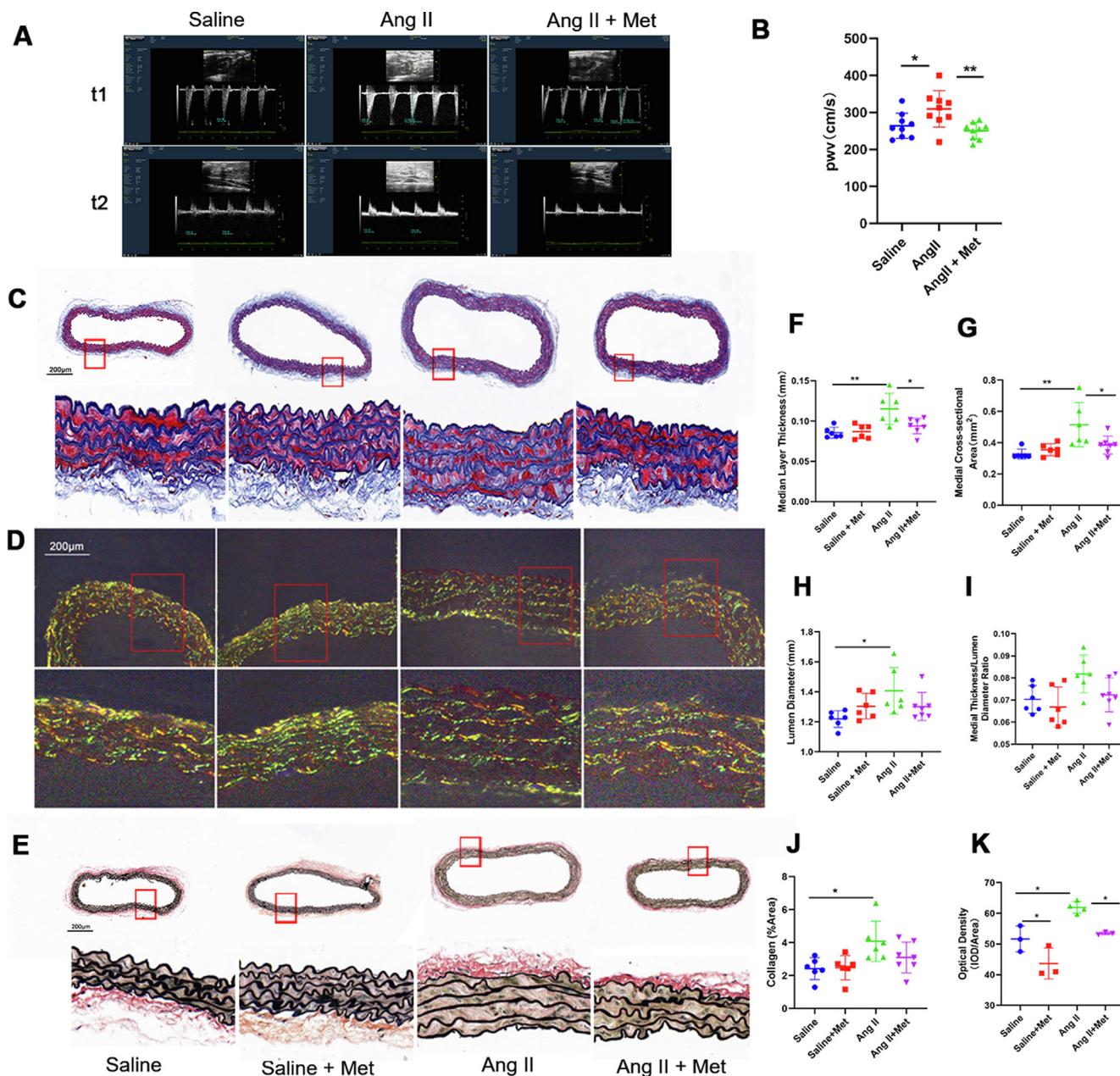
Fig. 2. Metformin alleviates functional and structural alterations during vascular senescence. PWV measurement represents a valid tool for noninvasively quantifying arterial stiffness. **A and B**, PWV was higher in Ang II-infused mice in comparison with age-matched control animals, while metformin administration decreased PWV in comparison with the Ang II-infusion group (one-way ANOVA, Tukey post hoc; n = 9). Alterations to collagen and elastin contents as well as aortic wall arrangement were assessed by Masson's Trichrome, Picrosirius Red, and Van Gieson's staining of aortic tissue ring samples. **C**, Morphometric assessment of the four mouse groups after Masson's trichrome staining. **F, G, H, I, and J,** Medial layer thicknesses, medial cross-sectional areas, lumen diameters, medial thickness/lumen diameter ratios, and collagen levels were calculated (one-way ANOVA, Tukey post hoc; n = 6–7). Scale bar = 200 μm. **D and K,** Circularly polarized light detection of collagen fibers, with collagen contents obtained within randomly selected fields. Optical density was determined (one-way ANOVA, Tukey post hoc; n = 3). Scale bar = 200 μm. **E**, Elastin fibers were detected by Van Gieson's staining; scale bar = 200 μm. Data are mean ± SD. *P < 0.05, **P < 0.01, and ***P < 0.001 versus control group or for indicated comparisons. PWV, pulse wave velocity.

(Fig. 2C and G). Collagen fiber visualization was performed under circularly polarized light (Fig. 2D), and collagen levels were obtained. Interestingly, collagen content and density were significantly elevated in the Ang II-infusion group, and metformin alleviated such effects (Fig. 2D, J, and K). Overtly thinner and fewer elastin fibers were observed in the Ang II-infusion group; however, metformin treatment could relieve the elastin fiber damage (Fig. 2E). Taken together, these data suggested that metformin alleviated the structural changes occurring during the process of vascular senescence.

Metformin reduces SASP in senescent VSMCs

In order to assess metformin's function in cell senescence, senescent primary VSMCs from the aortas of elderly patients were isolated (Supplementary Fig. 2) and treated with metformin. Surprisingly, SA-β-gal-positive cells were remarkably less abundant following metformin administration (Fig. 3A and C). These results were further confirmed by Western blot, which showed that metformin significantly decreased p53, p21, and p16 protein levels in primary VSMCs (Fig. 3B and C). Moreover, Ang II-induced
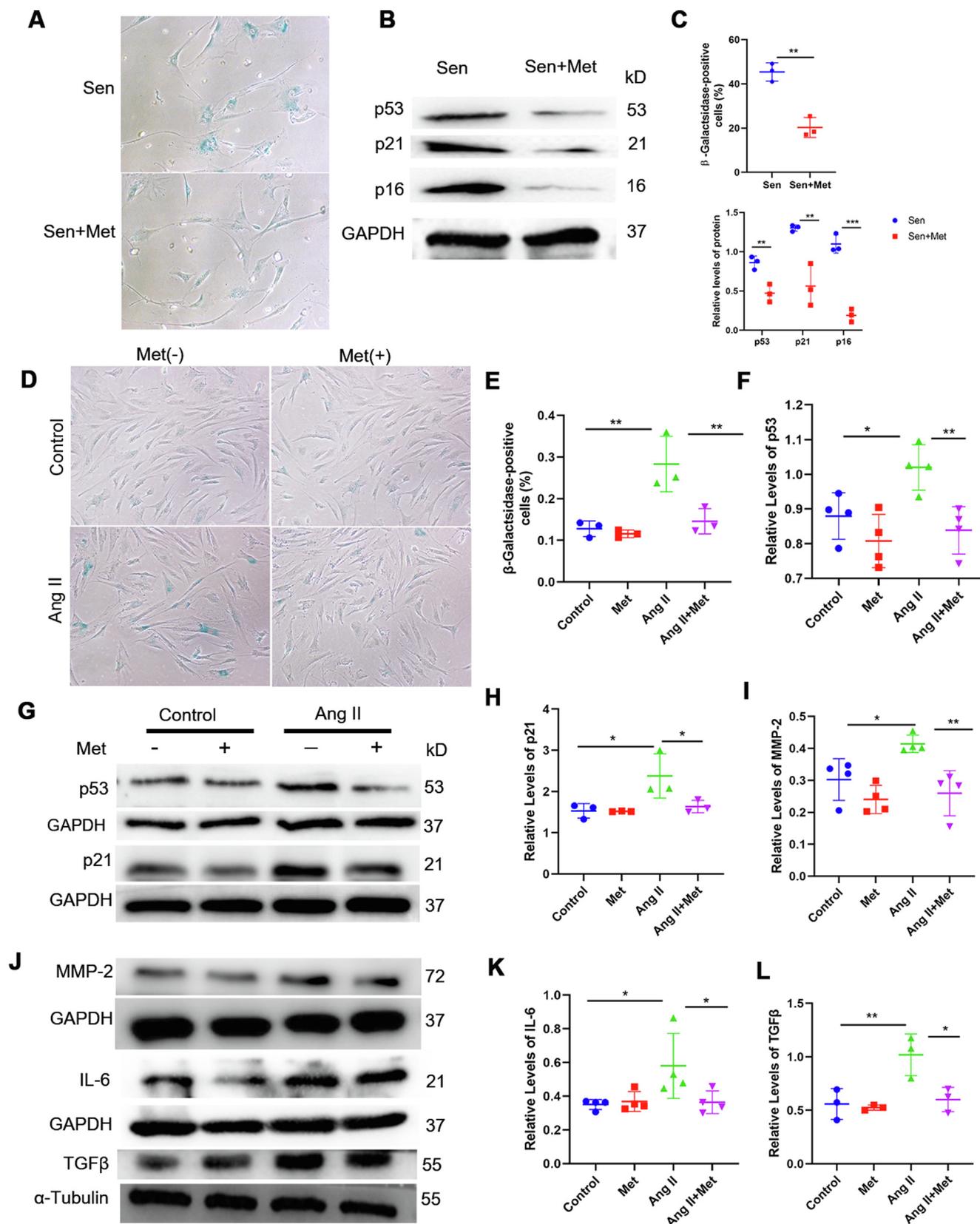
Fig. 3. Metformin treatment delays cellular senescence and alleviates the SASP of VSMCs. Senescent primary VSMCs from the aortas of elderly patients were used to examine metformin's effect on cellular senescence. **A, B and C**, The number of SA-β-gal-positive cells as well as p53, p21, and p16 protein levels were decreased by metformin treatment (*t*-test, n = 3). Ang II-induced premature senescent VMSCs were treated with metformin for further confirm its beneficial effects in cellular senescence. **D and E**, SA-β-gal staining was carried out for examining senescence in VSMCs (one-way ANOVA, Tukey post hoc; n = 3). **F, G, and H,** Immunoblot was carried out to determine p53 and p21 protein levels in Ang II-induced senescent VSMCs. GAPDH was utilized for normalization (one-way ANOVA, Tukey post hoc; n = 3–4). **I, J, K, and L,** SASP markers in Ang II-induced senescent VSMCs, including MMP-2, IL-6, and TGF-β, were further assessed by immunoblot. GAPDH was utilized for MMP-2 and IL-6 level normalization, and α-tubulin was used for TGF-β level normalization (one-way ANOVA, Tukey post hoc; n = 3–4). Data are mean ± SD. *P < 0.05, **P < 0.01, and ***P < 0.001 versus control group or for indicated comparisons.

premature senescent VMSCs were treated with metformin for further confirming metformin's beneficial effects in cell senescence. As expected, the number of SA-β-gal-positive cells was starkly higher after VSMC treatment with Ang II compared with the control group, while metformin treatment remarkably reduced the number of SA-β-gal-positive cells in comparison with the Ang II group (Fig. 3D and E). Consistently, immunoblot demonstrated that p53 and p21 protein levels were increased in Ang II-induced senescent VSMCs but reduced in the Ang II + metformin group (Fig. 3F, G, and H). Senescent VSMCs with the SASP contribute towards enhanced vascular inflammation and worsened disease condition through pro-inflammatory factors and ECM-damaging substances. Ang II-induced premature senescence enhanced the secretion of MMP2, IL-6, and TGF-β, and this effect was inhibited by metformin (Fig. 3I, J, K, and L). Collectively, these results suggested that metformin treatment delayed the development of cellular senescence and alleviated the SASP of VSMCs.

Given that cellular senescence mostly features cell-cycle arrest after continuous stimulation [13], we examined the effects of metformin on the biological characteristics of VSMCs with both basal and senescent statuses. The wound-healing assay revealed that metformin not only increased cell migration under basal conditions but also promoted the migration of Ang II-treated cells (Fig. 4A and C), suggesting that metformin reverses the decreased migration in senescent VSMCs. We next examined the phenotype of VSMCs, which showed increased levels of the proliferation-related protein PCNA, as well as decreased levels of the contractile proteins SM-22α and calponin, after treatment with metformin under both basal and senescent conditions (Fig. 4B and D-F). In order to further examine whether metformin-treatment influences cell growth arrest in senescent VSMCs, flow cytometry was performed. As shown in Fig. 4G-H, G0/G1 cell-cycle arrest was markedly elevated in Ang II-induced senescent cells, and these effects were alleviated following metformin treatment. Metformin prolonged the S phase, which was inhibited by Ang II treatment. Thus, metformin may promote the conversion of VSMCs from growth arrest and quiescence into an activated cell-cycle state. Collectively, these results suggested that metformin exerted beneficial effects by restoring the function of senescent VSMCs.

Autophagy is involved in the beneficial effects of metformin against senescence

Next, we explored the mechanism underlying the anti-senescence effects of metformin. Proteome analysis of aorta specimens from metformin-treated mice revealed 202 upregulated and 252 downregulated proteins, with statistical significance (fold change > 1.2 or < 0.83) (Fig. 5A). In order to further examine metformin's role in the aging vasculature, Gene Ontology (GO) and Clusters of Orthologous Groups of proteins (COG) analyses were carried out. Corroborating previously reported findings [1], metformin's target proteins were markedly enriched in catalytic activity, posttranslational modification, protein turnover, and chaperones, all of which are closely associated with the autophagic process (Fig. 5B-C).

Increasing evidence indicates reduced autophagy in vascular damage and increased susceptibility to vascular diseases during aging; [21] therefore, we examined autophagy levels in the vascular tissue using a transmission electron microscope (TEM, Hitachi7700, Japan), immunofluorescence staining, and Western blot. TEM revealed fewer autophagosome-like structures in aorta samples from the Ang II-infusion mouse group compared with control mice, but markedly more in metformin-treated animals (Fig. 5D and E). Although autophagosome levels were comparable in Ang II-infused animals with and without metformin treatment, more autophagosomes were observed in Ang II-infused animals admin-

istered metformin. Immunofluorescence further demonstrated that mice stimulated with Ang II infusion had LC3 II downregulation in comparison with control mice, while those treated with Ang II infusion and metformin showed significant upregulation of LC3 II in comparison with Ang II-infused mice (Fig. 5F and G). LC3 assessment does not differentiate autophagy flux activation from its impairment. In this study, p62 was overtly downregulated in Ang II-infused animals treated with metformin in comparison with the Ang II-infusion group, as demonstrated by immunofluorescence and immunoblot. Although LC3II abundance tended to increase in metformin-treated mice, the LC3II/I ratio showed no significant differences between Ang II-infused animals with and without metformin treatment (Fig. 5H, I, and J). Taken together, the above findings suggested metformin's beneficial effects in senescence may partly involve autophagy induction.

Metformin upregulates autophagic flux in the aging vasculature and senescent VSMCs

In order to confirm the above results obtained in mice, the effect of metformin on autophagy was examined *in vitro*. Consistent with the *in vivo* findings, significant p62 accumulation was observed after Ang II treatment, which was strongly decreased by intervention with metformin. Nevertheless, p62 protein levels were not affected by metformin under basal conditions. Interestingly, metformin treatment reduced the LC3II/I ratio under both basal and senescent conditions (Fig. 6A, B, and C); these effects could be blocked by autophagy inhibition using bafilomycin A1, a vacuolar-type H$^+$-ATPase that inhibits autolysosome function (Fig. 6D and E). Since metformin acts via the AMPK/mTOR pathway in attenuating hallmarks of biological aging, we assessed AMPK protein and phosphorylation levels in senescent primary VSMCs treated with or without metformin (Fig. 6 F and G). The results showed that AMPK protein and phosphorylation levels were not affected by metformin, suggesting the anti-senescence effects of metformin in senescent VSMCs were independent of the AMPK pathway, and the initiation of autophagy may not be affected by metformin in senescent VSMCs.

Metformin enhances autophagy flux at the autophagosome-lysosome fusion level

Autophagy involves several events regulated on multiple levels. Our observation that metformin reduces p62 in senescent VSMCs, corresponding to increased autophagy (Fig. 6H), is contradictory to the finding of decreased LC3II/I ratio, which suggests autophagy disruption. In order to further explore the molecular mechanism underlying the effects of metformin on autophagy, changes in multiple autophagy-related proteins were screened by proteomics. Bioinformatic analysis hinted at the role of elevated lysosome-associated membrane protein 1 (LAMP1) in the autolysosome formation process. We thus tested whether LAMP1 expression was significantly upregulated post-metformin treatment. As expected, we found increased LAMP1 protein levels (Fig. 6J and K) in Ang II-induced senescent VSMCs treated with metformin. In addition, immunohistochemical staining of aortas revealed that the old + metformin mice displayed increased LAMP1 levels compared wtih the old mice (Supplementary Fig. 3A). Similar results were observed in aortas from the Ang II infusion + metformin mice (Supplementary Fig. 3B). Given that LAMP1 is a biomarker of degrading autophagy-associated lysosomes [34], we stained autolysosomes to observe the effect of metformin on autophagic flux (Fig. 6H). As expected, Ang II stimulation significantly suppressed autolysosome formation, whereas metformin reversed Ang II-induced suppression of autolysosome formation. Additionally, lysosome function blockade with bafilomycin A1 significantly decreased
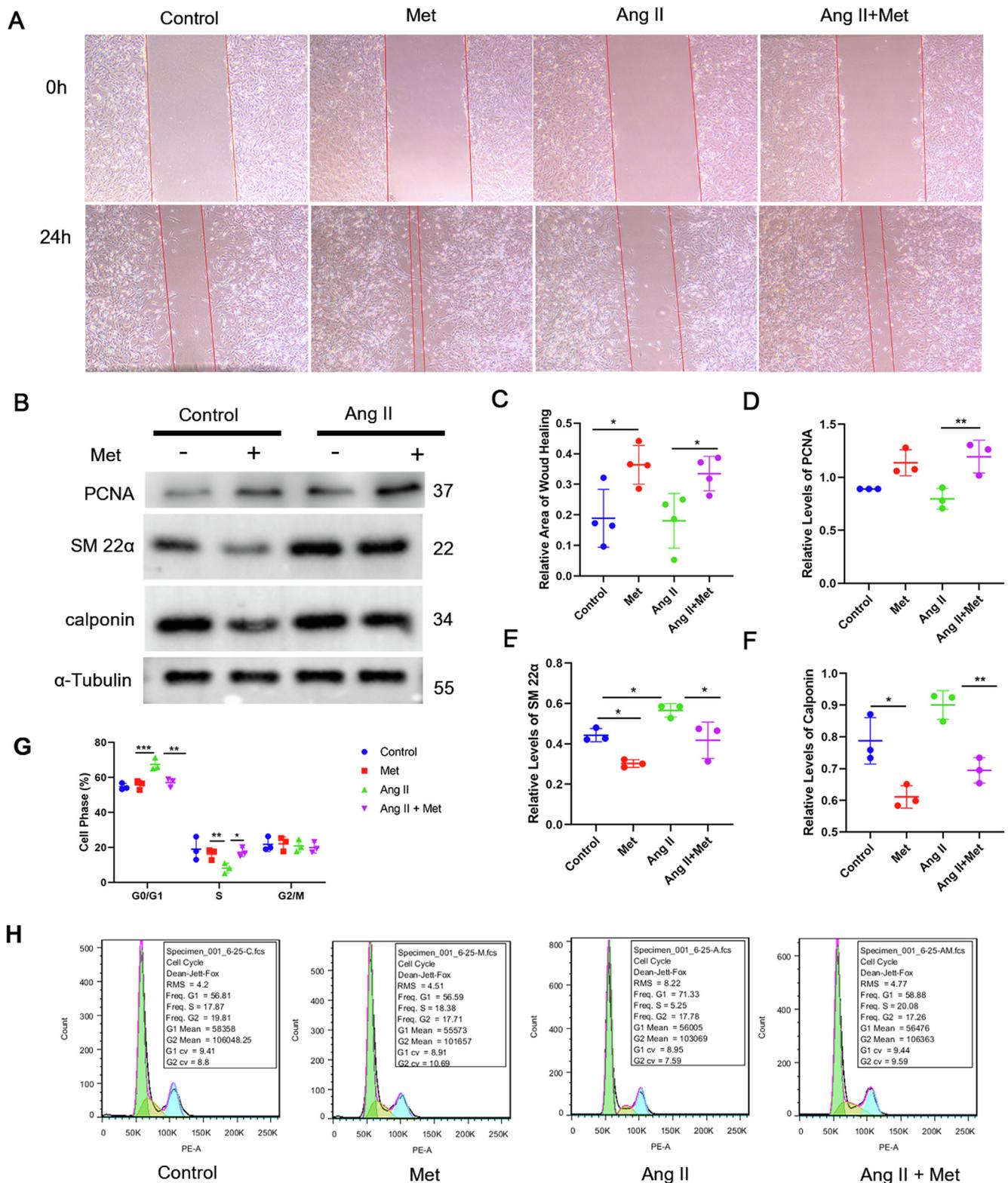
Fig. 4. Metformin has beneficial effects on function restoration in senescent VSMCs. The migration of Ang II-induced senescent VSMCs was determined by the wound-healing assay. **C**, Semi-quantitative analysis of wound area healing at a fixed location was performed with Image J. VSMCs underwent incubation with or without Ang II (2 μM) for 24 h with metformin (200 μM) treatment or not (one-way ANOVA, Tukey post hoc; n = 4). **B, D, E, and F,** The expression levels of PCNA, SM-22α, and calponin in Ang II-induced senescent VSMCs were assessed by immunoblot, using α-tubulin for normalization (one-way ANOVA, Tukey post hoc; n = 3). **G-H**, Flow cytometry showed G0/G1 cell-cycle arrest was increased significantly in Ang II-treated cells, and this effect was alleviated by metformin treatment, while metformin increased S phase cells that were inhibited by Ang II treatment (one-way ANOVA, Tukey post hoc; n = 3). Data are mean ± SD. *$P < 0.05$, **$P < 0.01$, and ***$P < 0.001$ versus control group or for indicated comparisons.
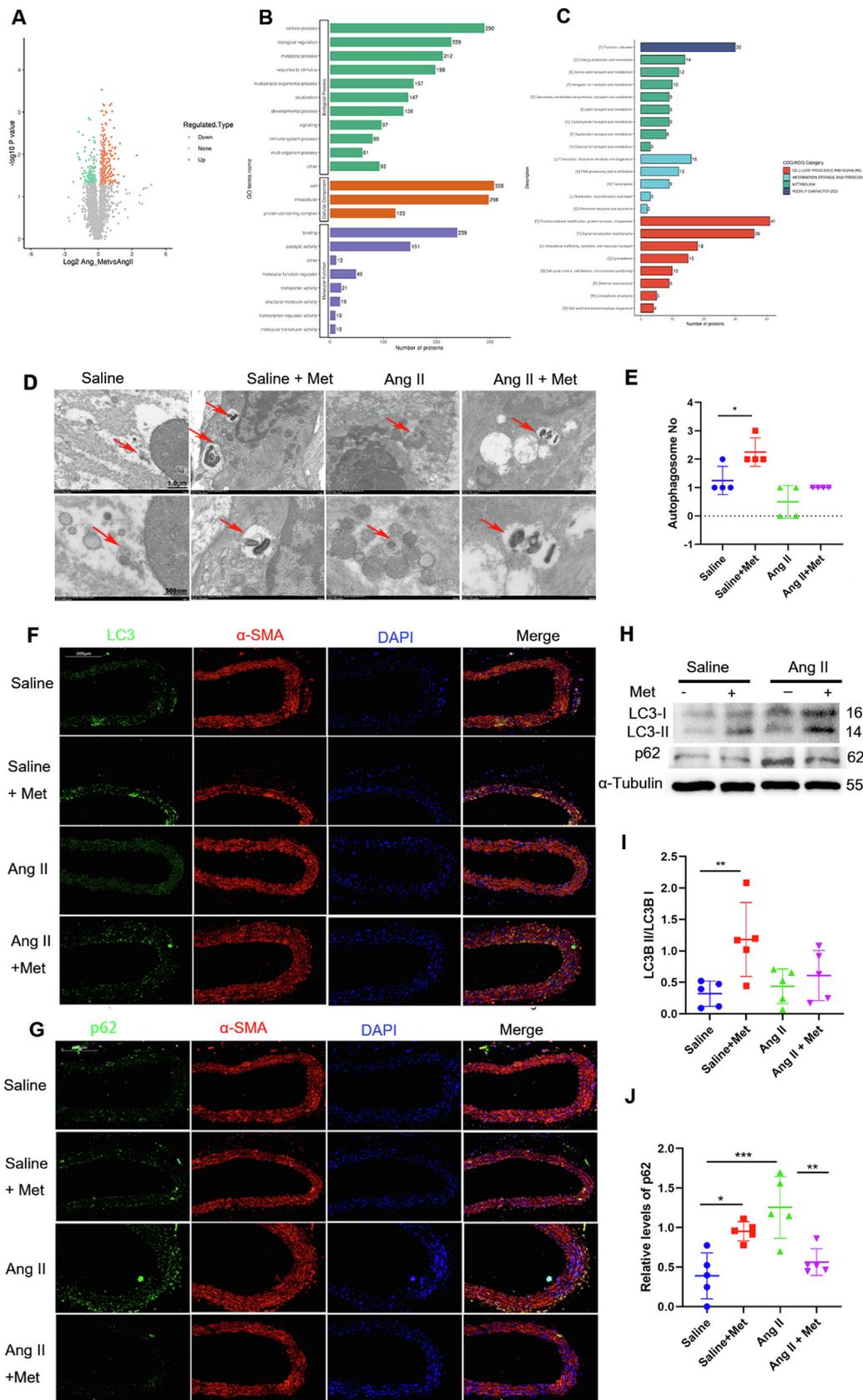
Fig. 5. Autophagy contributes to metformin's beneficial effects in senescence. A, Proteomics of aorta specimens from metformin-treated mice revealed 202 upregulated and 252 downregulated proteins, with statistical significance. **B and C**, GO and COG analyses showed metformin's targets were markedly enriched in catalytic activity, posttranslational modification, protein turnover, and chaperones. **D and E**, The autophagosome levels in aorta specimens from the 4 groups were examined by TEM (one-way ANOVA, Tukey post hoc; n = 4). Scale bar = 1.0 μm (upper panel) or 500 nm (lower panel). **F and G**, LC3, and p62 levels in aorta samples were assessed by immunofluorescence; α-SMA was simultaneously stained to confirm the location of VSMCs. **H, I, and J**, Immunoblot assessment of LC3 and p62 in aorta specimens, with α-tubulin used for normalization (one-way ANOVA, Tukey post hoc; n = 5). Data are mean ± SD. *P < 0.05, **P < 0.01, and ***P < 0.001 versus control group or for indicated comparisons.
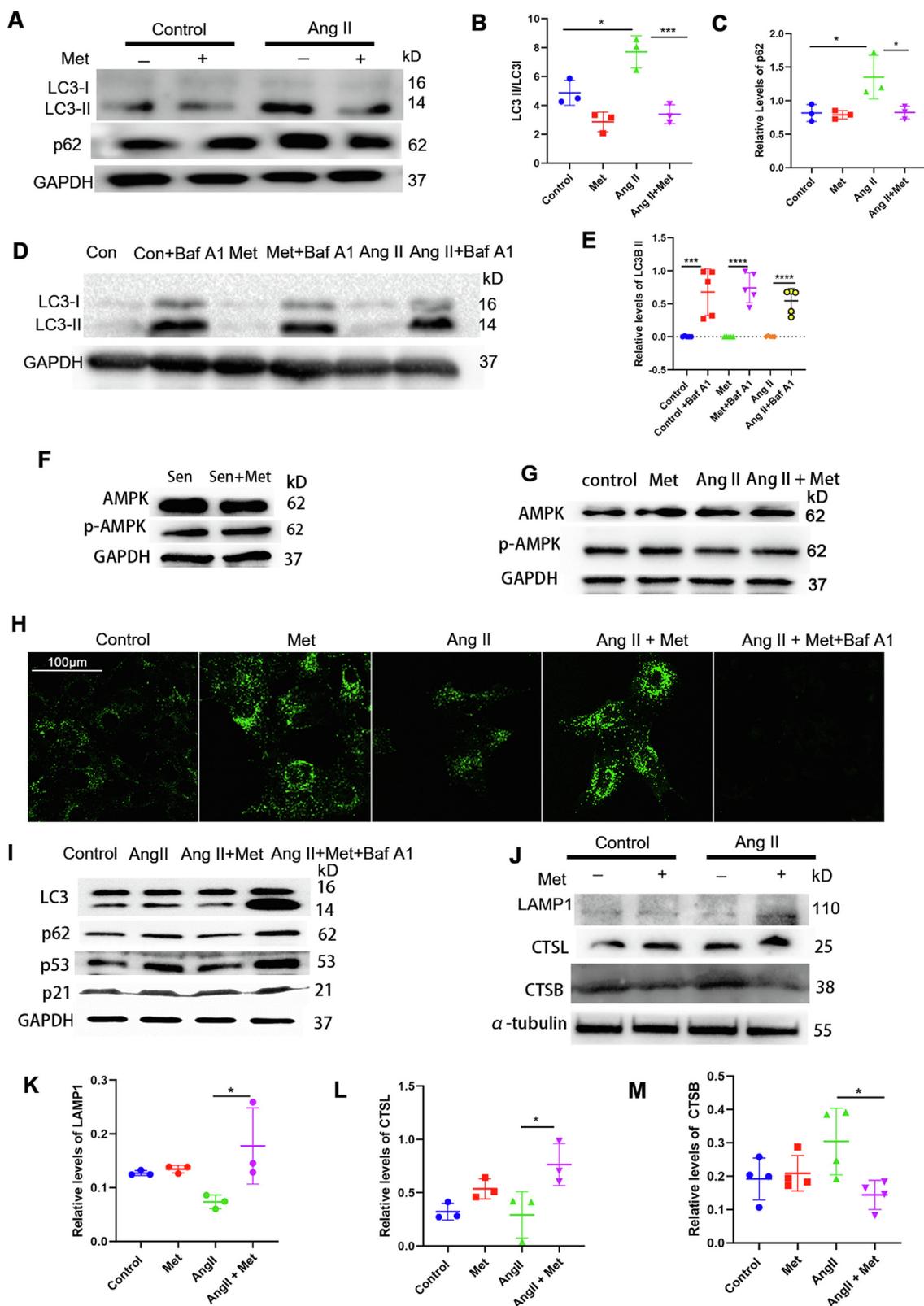
Fig. 6. Metformin promotes autophagic flux at the autophagosome-lysosome fusion level. A, B, and C, The expression levels of LC3 and p62 in Ang II-induced senescent VSMCs were examined by immunoblot. VSMCs underwent incubation in the presence or absence of Ang II (2 μM) for 24 h, with metformin (200 μM) treatment or not. GAPDH was utilized for normalization (one-way ANOVA, Tukey post hoc; n = 3). **D and E**, To inhibit autophagy, VSMCs were incubated with bafilomycin A1, then treated with metformin and Ang II; LC3 protein levels were assessed by immunoblot, with GAPDH as a loading control (one-way ANOVA, Tukey post hoc; n = 5). **F and G**, AMPK protein, and phosphorylation levels were evaluated by immunoblot in senescent primary VSMCs treated or not with metformin. **H,** To evaluate metformin's effect on autophagic flux, autolysosome staining was performed; scale bar = 100 μm. **I**, VSMCs was pre-incubated with bafilomycin A1 for two hours, then treated with metformin and Ang II; LC3, p62, p53, and p21 protein levels were evaluated by immunoblot. **J-M,** LAMP1, CSTL, CSTB protein levels were examined by immunoblot (one-way ANOVA, Tukey post hoc; n = 3–4). Data are mean ± SD. *P < 0.05, **P < 0.01, and ***P < 0.001 versus control group or for indicated comparisons. Baf A1, bafilomycin A1.

autolysosome formation. Cathepsin L (CTSL) positively regulates lysosomal function since it increases autophagy and lysosomal activity. Increased CTSL protein levels were observed in Ang II-induced senescent VSMCs administered metformin (Fig. 6J and L). Meanwhile, the protein levels of Cathepsin B (CTSB), a pro-apoptotic enzyme and a negative regulator of lysosomal function were reduced in Ang II-induced senescent VSMCs administered metformin (Fig. 6J and M). Next, Ang II-induced senescent VSMCs were administered metformin and incubated with or without bafilomycin A1, which reversed the anti-senescence effects of metformin (Fig. 6 I). Given the autophagy receptor sqstm1/p62 (sequestosome 1) serve as a major regulator of autophagy involved in the targeting of cargo into autophagosomes [35], Ad-sqstm1/p62-RNAi was used to further test the effect and mechanism of metformin on modulating autophagy flux in VSMCs. Consistent with a previous report [20], Ad-sqstm1/p62-RNAi significantly reduced p62 protein expression compared with Ad-control-treated cells while decreased LC3II abundance and increased p53 and p21 levels (Supplementary Fig. 4 and Supplementary Fig. 5). After sqstm1/p62 silencing, p53 and p21 expression was not affected by metformin. These data indicated that metformin promoted autophagy by enhancing autophagosome-lysosome fusion and ameliorated cellular and vascular senescence by prompting autophagosome formation.

Discussion

Beyond glycemic control in diabetics, epidemiological, animal, and human studies have suggested that metformin could be used as an anti-aging agent [36]. Metformin exerts various therapeutic effects on dysregulated nutrient sensing, genomic instability, proteostasis collapse, and reduced intercellular communication [1]. Despite broad application and demonstrated efficacy, how metformin modulates major pathways contributing to cellular and vascular senescence remains largely unclear. This study confirmed that metformin prevented senescence in VSMCs and the aging vasculature and also demonstrated that metformin could reduce the accumulation of senescence-associated secretory factors in VSMCs. Most importantly, we showed that metformin prompted autophagosome formation, which might be the main mechanism underlying the anti-aging effects of metformin in senescent VSMCs and aging vasculature. This study firstly reported the molecular mechanism of metformin in terms of promoting autophagosome formation possibly by upregulating LAMP1 in senescent VSMCs and the aging vasculature.

Cell senescence constitutes an important aging process that features irreversible growth arrest, impaired functions, and substantial changes in the proinflammatory secretome [37]. Previous evidence suggests eliminating senescent cells expressing p16^{INK4A} may extend the lifespan and improve health in mice [14,38], indicating a major role for cell senescence in aging-related physiological decline. Moreover, a recent study showed that senescent liver sinusoid endothelial cells are not replaced upon removal and play major structural and functional roles in aging organisms [15]. Thus, delaying senescence or replacing senescent cells using drugs such as metformin could represent a powerful tool for slowing down aging. During growth arrest associated with senescence, two core senescence-regulating pathways, including p53/p21 and p16^{INK4a}/Rb [39,40], play critical roles in the activation of downstream factors in retinoblastoma [41,42], irreversibly arresting the cell cycle [43]. Hence, elevated SA-β-gal activity and increased p53 and p21 levels are accepted markers of senescent cells. In this study, metformin restored vascular senescence, with reduced SA-β-gal activity and decreased p53 and p21 protein expression. Consistently, metformin significantly reduced Ang II-dependent

VSMC senescence *in vivo* and improved vascular wall thickening and collagen accumulation. Interestingly, metformin administration also caused fibrotic area and wall thickness reductions in the mouse aorta in comparison with the Ang II infusion group, suggesting that metformin prevents Ang II-induced remodeling in the mouse aorta. Taken together, these data suggest that metformin may effectively target vascular aging and prevent senescence in VSMCs.

Senescent vascular cells display elevated levels of reactive oxygen species and acquire the SASP, characterized by increased inflammatory cytokine and chemokine production. Senescent cells can also impact the functions and phenotypes of surrounding vascular cells via multiple different pathways. Age-associated arterial dysfunction and changes feature higher large elastic arterial stiffness and endothelial dysfunction, which represent important risk factors for cardiovascular disease and contribute towards various pathophysiologically relevant conditions [44]. With aging, collagen accumulation and vascular remodeling progressively increase, which can lead to arterial stiffness [33,45], further exacerbating endothelial dysfunction [33]. Cellular senescence is correlated with arterial remodelling [46], and its inhibition has been shown to ameliorate arterial stiffness in mice [47]. Moreover, resveratrol treatment was reported to prevent age-related vascular remodeling by inhibiting cellular senescence [48]. A previous study revealed that senescence-associated secretory factors derived from senescent VSMCs are negative mediators of arterial remodeling that promote TGF-β activation, induce collagen deposition, and increase wall-to-lumen ratios and blood pressure. In this study, metformin treatment decreased senescence and SASP in VSMCs and enhanced migration and proliferation in senescent VSMCs. Hence, we speculate that metformin may ameliorate vascular remodeling by suppressing senescence and the SASP in VSMCs. In contrast to our study, data from another study indicated that Ang II effectively promotes VSMC migration at 48 h, while metformin inhibits this effect[8]. The divergent result may be explained by the different doses of metformin. A previous study [49] found that metformin dose-dependently regulates the biological properties of periodontal ligament stem cells (PDLSCs) *in vitro*. The results showed that maximal effect was achieved with 50 μM metformin treatment, which significantly increased the proliferation and migration of PDLSCs. In addition, 10 mM metformin was used in the study mentioned above[8], whereas in our study 200 μM metformin was administrated. To verify the hypothesis that metformin at a lower dose could increase VSMC growth, while metformin at a higher dose might result in opposite effects, the dose–response experiments of metformin (0 μM, 50 μM, 200 μM, 1 mM, 5 mM, 10 mM) on VSMCs were performed. As shown in Supplementary Fig. 6, 50 μM and 200 μM metformin promoted VSMC growth in both basal and Ang II incubated conditions, whereas VSMC growth was obviously slowed down after incubation with 1 mM and 5 mM metformin. Importantly, excessive VSMC death was observed when incubated with 10 mM metformin. These results indicated that low-dose metformin, as the dose used in our study setting, would promote VSMC growth, and the opposite effect was observed by high-dose metformin. Moreover, Western blot demonstrated that LC3 II abundance tended to decrease in VSMC treated with 1 mM and 5 mM metformin when compared with 50 μM and 200 μM metformin treatment. Taken together, it is reasonable to speculate that the divergent results in terms of metformin on VSMC proliferation and migration might be contributed to the various doses used. However, the exact underpinning mechanism deserves further investigation.

Unlike senescent growth arrest, the SASP does not depend on p53 or p16^{INK4a} [43]; it develops relatively slowly and usually takes several days to manifest after senescent growth arrest has been initiated. Autophagy is a complex and dynamic intracellular process

that delivers cytoplasmic constituents into lysosomes for degradation [50], which is essential for cell survival and the phenotype of smooth muscle cells [51]. Impaired autophagy has been reported to stimulate senescence, while autophagy is also involved in SASP establishment [20]. Here, we found that metformin did not initiate autophagy but rather promoted autophagic flux, whereas metformin might affect lysosomal fusion with autophagosomes possibly via LAMP1 mediation. Indeed, we observed that metformin treatment was associated with increased LAMP1 protein levels and enhanced autolysosome formation. It is worth noting that LAMP1 and CSTL/B in the Ang II vs. control groups were not statistically significant in our study. The effect of Ang II on VSMC autophagy might be dose-dependent, in that autophagy could be stimulated by Ang II at a lower dose, while inhibited with Ang II at a higher dose. According to a previous report, Ang II at lower concentrations between 10 and 100 nM stimulated autophagy in the HL-1 cardiomyocyte cell line, whereas higher concentrations caused apoptosis and decreased autophagy [52]. We used a high dose of Ang II in our study, which was thus linked with decreased autophagy. We speculate that autophagy is a multi-step and complex process, Ang II may not directly influence autophagy by regulating lysosomes, while metformin might improve effective autophagy by regulating activities of lysosomes. Here, we demonstrated that downregulating lysosomal function by bafilomycin A1 increased p21 and p53 expression as well as SA-β-gal activity in response to Ang II. Moreover, bafilomycin A1 abrogated metformin's beneficial effects against senescence in VSMCs. Jointly, the above findings indicate the anti-senescence effects induced by metformin are at least partly mediated by autophagy promotion and lysosome function enhancement. This study shows that metformin could prevent defective autophagy during the development of senescence and alleviate SASP in VSMCs. Still, future studies using various autophagy antibodies working on different stages of autophagy are needed to verify the exact working mechanism of metformin on modulating the autophagy process.

Clinical implications

Previous studies provided compelling evidence that vascular aging represents a major player in overall organismal aging [53,54]. More recently, a study suggested that modulating the vascular endothelial growth factor pathway may result in increased mammalian lifespan [55]. The current results provide evidence of metformin's beneficial effects against vascular and cellular senescence and the associated mechanisms. Taken together, these findings demonstrate the potential of metformin as a candidate agent to prevent vascular aging.

Conclusions

This study demonstrated that metformin ameliorates cellular and vascular senescence via suppression of the secretion of senescence-associated factors by promoting autophagic flux. This work identified discrete anti-senescence targets of metformin on senescent VSMCs independent of diabetic control; future studies are warranted to determine whether metformin is beneficial for patients with vascular diseases and slows down vascular aging independently of the presence of diabetes.

Funding

Declaration of Competing Interest

The authors declare that they have no known competing financial interests or personal relationships that could have appeared to influence the work reported in this paper.

Acknowledgments

Appendix A. Supplementary data

Supplementary data to this article can be found online at https://doi.org/10.1016/j.jare.2021.12.009.

References

[1] Kulkarni AS, Gubbi S, Barzilai N. Benefits of metformin in attenuating the hallmarks of aging. Cell. Metab. 2020;32(1):15–30.

[2] Xu M, Pirtskhalava T, Farr JN, Weigand BM, Palmer AK, Weivoda MM, et al. Senolytics improve physical function and increase lifespan in old age. Nat. Med. 2018;24(8):1246–56.

[3] Kulkarni AS, Brutsaert EF, Anghel V, Zhang K, Bloomgarden N, Pollak M, et al. Metformin regulates metabolic and nonmetabolic pathways in skeletal muscle and subcutaneous adipose tissues of older adults. Aging Cell 2018;17(2): e12723. doi: https://doi.org/10.1111/acel.2018.17.issue-210.1111/acel.12723.

[4] Justice JN, Nambiar AM, Tchkonia T, LeBrasseur NK, Pascual R, Hashmi SK, et al. Senolytics in idiopathic pulmonary fibrosis: Results from a first-in-human, open-label, pilot study. EBioMedicine. 2019;40:554–63.

[5] Fang J, Yang J, Wu X, Zhang G, Li T, Wang Xi'e, et al. Metformin alleviates human cellular aging by upregulating the endoplasmic reticulum glutathione peroxidase 7. Aging Cell 2018;17(4):e12765. doi: https://doi.org/10.1111/acel.2018.17.issue-410.1111/acel.12765.

[6] Bharath LP, Agrawal M, McCambridge G, Nicholas DA, Hasturk H, Liu J, et al. Metformin enhances autophagy and normalizes mitochondrial function to alleviate aging-associated inflammation. Cell Metab. 2020;32(1):44–55.e6.

[7] Kunath A, Unosson J, Friederich-Persson M, Bjarnegård N, Becirovic-Agic M, Björck M, et al. Inhibition of angiotensin-induced aortic aneurysm by metformin in apolipoprotein E-deficient mice. JVS Vasc. Sci. 2021;2:33–42.

[8] Wang Z, Guo J, Han X, Xue M, Wang W, Mi L, et al. Metformin represses the pathophysiology of AAA by suppressing the activation of PI3K/AKT/mTOR/ autophagy pathway in ApoE(-/-) mice. Cell. Biosci. 2019;9(1). doi: https://doi.org/10.1186/s13578-019-0332-9.

[9] Zhou D-M, Ran F, Ni H-Z, Sun L-L, Xiao Li, Li X-Q, et al. Metformin inhibits high glucose-induced smooth muscle cell proliferation and migration. Aging (Albany NY). 2020;12(6):5352–61.

[10] Herranz N, Gil J. Mechanisms and functions of cellular senescence. J. Clin. Invest. 2018;128:1238–46.

[11] He S, Sharpless NE. Senescence in health and disease. Cell 2017;169 (6):1000–11.

[12] Lin C, Li H, Liu J, Hu Q, Zhang S, Zhang Na, et al. Arginine hypomethylation-mediated proteasomal degradation of histone H4-an early biomarker of cellular senescence. Cell. Death Differ. 2020;27(9):2697–709.

[13] Tchkonia T, Zhu Yi, van Deursen J, Campisi J, Kirkland JL. Cellular senescence and the senescent secretory phenotype: therapeutic opportunities. J. Clin. Invest. 2013;123(3):966–72.

[14] Baker DJ, Childs BG, Durik M, Wijers ME, Sieben CJ, Zhong J, et al. Naturally occurring p16(Ink4a)-positive cells shorten healthy lifespan. Nature 2016;530 (7589):184–9.

[15] Grosse L, Wagner N, Emelyanov A, Molina C, Lacas-Gervais S, Wagner K-D, et al. Defined p16(high) senescent cell types are indispensable for mouse healthspan. Cell. Metab. 2020;32(1):87–99.e6.

[16] Ungvari Z, Tarantini S, Sorond F, Merkely B, Csiszar A. Mechanisms of vascular aging, a geroscience perspective: JACC focus seminar. J. Am. Coll. Cardiol. 2020;75(8):931–41.

[17] Childs BG, Gluscevic M, Baker DJ, Laberge R-M, Marquess D, Dananberg J, et al. Senescent cells: an emerging target for diseases of ageing. Nat. Rev. Drug Discov. 2017;16(10):718–35.

[18] Grootaert MOJ, da Costa Martins PA, Bitsch N, Pintelon I, De Meyer GRY, Martinet W, et al. Defective autophagy in vascular smooth muscle cells accelerates senescence and promotes neointima formation and atherogenesis. Autophagy. 2015;11(11):2014–32.

[19] M.O.J. Grootaert, M. Moulis, L. Roth, W. Martinet, C. Vindis, M.R. Bennett, G.R.Y. De Meyer, Vascular smooth muscle cell death, autophagy and senescence in atherosclerosis, Cardiovasc. Res. 2018;114:622-634.

[20] Salazar G, Cullen A, Huang J, Zhao Y, Serino A, Hilenski L, et al. SQSTM1/p62 and PPARGC1A/PGC-1alpha at the interface of autophagy and vascular senescence. Autophagy 2020;16(6):1092–110.

[21] Abdellatif M, Sedej S, Carmona-Gutierrez D, Madeo F, Kroemer G. Autophagy in cardiovascular aging. Circ. Res. 2018;123(7):803–24.

[22] Ren J, Zhang Y. Targeting autophagy in aging and aging-related cardiovascular diseases. Trends Pharmacol. Sci. 2018;39(12):1064–76.

[23] Chandel N, Avizonis D, Reczek C, Weinberg S, Menz S, Neuhaus R, et al. Are metformin doses used in murine cancer models clinically relevant? Cell. Metab. 2016;23(4):569–70.

[24] Chirinos JA, Segers P, Hughes T, Townsend R. Large-artery stiffness in health and disease: JACC state-of-the-art review. J. Am. Coll. Cardiol. 2019;74:1237–63.

[25] Reddy AK, Li Y-H, Pham TT, Ochoa LN, Treviño MT, Hartley CJ, et al. Measurement of aortic input impedance in mice: effects of age on aortic stiffness. Am. J. Physiol. Heart Circ. Physiol. 2003;285(4):H1464–70.

[26] Sehgel NL, Sun Z, Hong Z, Hunter WC, Hill MA, Vatner DE, et al. Augmented vascular smooth muscle cell stiffness and adhesion when hypertension is superimposed on aging. Hypertension 2015;65(2):370–7.

[27] Chi J, Meng L, Pan S, Lin H, Zhai X, Liu L, et al. Primary culture of rat aortic vascular smooth muscle cells: a new method. Med. Sci. Monit. 2017;23:4014–20.

[28] Nakano-Kurimoto R, Ikeda K, Uraoka M, Nakagawa Y, Yutaka K, Koide M, et al. Replicative senescence of vascular smooth muscle cells enhances the calcification through initiating the osteoblastic transition. Am. J. Physiol. Heart Circulatory Physiol. 2009;297(5):H1673–84.

[29] Li D-J, Huang F, Ni M, Fu H, Zhang L-S, Shen F-M. α7 nicotinic acetylcholine receptor relieves angiotensin ii-induced senescence in vascular smooth muscle cells by raising nicotinamide adenine dinucleotide-dependent SIRT1 activity. Arterioscler. Thromb. Vasc. Biol. 2016;36(8):1566–76.

[30] Day EA, Ford RJ, Smith BK, Mohammadi-Shemirani P, Morrow MR, Gutgesell RM, et al. Metformin-induced increases in GDF15 are important for suppressing appetite and promoting weight loss. Nat. Metab. 2019;1 (12):1202–8.

[31] Lu Y, Pechlaner R, Cai J, Yuan H, Huang Z, Yang G, et al. Trajectories of age-related arterial stiffness in chinese men and women. J. Am. Coll. Cardiol. 2020;75(8):870–80.

[32] Chen K, Zhou X, Sun Z. Haplodeficiency of klotho gene causes arterial stiffening via upregulation of scleraxis expression and induction of autophagy. Hypertension 2015;66(5):1006–13.

[33] Donato AJ, Machin DR, Lesniewski LA. Mechanisms of dysfunction in the aging vasculature and role in age-related disease. Circ. Res. 2018;123(7):825–48.

[34] Cheng X-T, Xie Y-X, Zhou B, Huang N, Farfel-Becker T, Sheng Z-H. Revisiting LAMP1 as a marker for degradative autophagy-lysosomal organelles in the nervous system. Autophagy. 2018;14(8):1472–4.

[35] Geisler S, Holmström KM, Skujat D, Fiesel FC, Rothfuss OC, Kahle PJ, et al. PINK1/Parkin-mediated mitophagy is dependent on VDAC1 and p62/SQSTM1. Nat. Cell. Biol. 2010;12(2):119–31.

[36] Glossmann H, Lutz OD. Metformin and aging: a review. Gerontology. 2019;65 (6):581–90.

[37] J. Gil, Cellular senescence causes ageing, Nat. Rev. Mol. Cell. Biol. 2019;20:388.

[38] Jeon OH, Kim C, Laberge R-M, Demaria M, Rathod S, Vasserot AP, et al. Local clearance of senescent cells attenuates the development of post-traumatic osteoarthritis and creates a pro-regenerative environment. Nat. Med. 2017;23 (6):775–81.

[39] Beausejour CM, Krtolica A, Galimi F, Narita M, Lowe SW, Yaswen P, et al. Reversal of human cellular senescence: roles of the p53 and p16 pathways. EMBO J. 2003;22:4212–22.

[40] Herbig U, Jobling WA, Chen BPC, Chen DJ, Sedivy JM. Telomere shortening triggers senescence of human cells through a pathway involving ATM, p53, and p21(CIP1), but not p16(INK4a). Mol. Cell. 2004;14(4):501–13.

[41] Narita M, Nuñez S, Heard E, Narita M, Lin AW, Hearn SA, et al. Rb-mediated heterochromatin formation and silencing of E2F target genes during cellular senescence. Cell 2003;113(6):703–16.

[42] Chicas A, Wang X, Zhang C, McCurrach M, Zhao Z, Mert O, et al. Dissecting the unique role of the retinoblastoma tumor suppressor during cellular senescence. Cancer Cell. 2010;17(4):376–87.

[43] Kang C, Xu Q, Martin TD, Li MZ, Demaria M, Aron L, et al. The DNA damage response induces inflammation and senescence by inhibiting autophagy of GATA4. Science 2015;349(6255). doi: https://doi.org/10.1126/science: aaa5612.

[44] Ding YN, Tang X, Chen HZ, Liu DP. Epigenetic regulation of vascular aging and age-related vascular diseases. Adv. Exp. Med. Biol. 2018;1086:55–75.

[45] Uddin MS, Kabir MT, Jakaria M, Mamun AA, Niaz K, Amran MS, et al. Endothelial PPARgamma is crucial for averting age-related vascular dysfunction by stalling oxidative stress and ROCK. Neurotox. Res. 2019;36:583–601.

[46] Kedenko L, Lamina C, Kedenko I, Kollerits B, Kiesslich T, Iglseder B, et al. Genetic polymorphisms at SIRT1 and FOXO1 are associated with carotid atherosclerosis in the SAPHIR cohort. BMC Med. Genet. 2014;15(1). doi: https://doi.org/10.1186/s12881-014-0112-7.

[47] Fry JL, Al Sayah L, Weisbrod RM, Van Roy I, Weng X, Cohen RA, et al. Vascular smooth muscle sirtuin-1 protects against diet-induced aortic stiffness. Hypertension 2016;68(3):775–84.

[48] Jang I-A, Kim E, Lim Ji, Kim M, Ban T, Yoon H, et al. Effects of resveratrol on the renin-angiotensin system in the aging kidney. Nutrients. 2018;10(11):1741. doi: https://doi.org/10.3390/nu10111741.

[49] Zhang R, Liang Q, Kang W, Ge S. Metformin facilitates the proliferation, migration, and osteogenic differentiation of periodontal ligament stem cells in vitro. Cell. Biol. Int. 2020;44(1):70–9.

[50] T.D. Evans, I. Sergin, X. Zhang, B. Razani, Target acquired: Selective autophagy in cardiometabolic disease, Sci. Signal. 2017;10

[51] De Munck DG, De Meyer GRY, Martinet W. Autophagy as an emerging therapeutic target for age-related vascular pathologies. Expert Opin. Ther. Targets. 2020;24(2):131–45.

[52] Forrester SJ, Booz GW, Sigmund CD, Coffman TM, Kawai T, Rizzo V, et al. Angiotensin II signal transduction: an update on mechanisms of physiology and pathophysiology. Physiol. Rev. 2018;98(3):1627–738.

[53] Ungvari Z, Tarantini S, Kiss T, Wren JD, Giles CB, Griffin CT, et al. Endothelial dysfunction and angiogenesis impairment in the ageing vasculature. Nat. Rev. Cardiol. 2018;15(9):555–65.

[54] Le Couteur DG, Lakatta EG. A vascular theory of aging. J. Gerontol. A Biol. Sci. Med. Sci. 2010;65A(10):1025–7.

[55] Grunewald M, Kumar S, Sharife H, Volinsky E, Gileles-Hillel A, Licht T, et al. Counteracting age-related VEGF signaling insufficiency promotes healthy aging and extends life span. Science 2021;373(6554). doi: https://doi.org/ 10.1126/science:abc8479.